Metabolic Brain Disease (2019) 34:1689–1703
https://doi.org/10.1007/s11011-019-00475-4

ORIGINAL ARTICLE

Combination of schisandrin and nootkatone exerts neuroprotective effect in Alzheimer's disease mice model

Yu Qi[1] · Xinhui Cheng[1] · Huiting Jing[1] · Tingxu Yan[2] · Feng Xiao[2] · Bo Wu[2] · Kaishun Bi[3] · Ying Jia[2]

Received: 7 May 2019 / Accepted: 28 July 2019 / Published online: 17 August 2019

Abstract

Alzheimer's disease (AD) is one of the most common neurodegenerative diseases which seriously affect the quality of life of the elderly. Schisandrin (SCH) and nootkatone (NKT) are the two marked active components in ASHP. In this study, the effects of *Alpinia oxyphylla—Schisandra chinensis* herb pair (ASHP) as well as its bioactive components on cognitive deficiency and dementia were revealed via $A\beta_{1-42}$-induced AD in mouse. Morris water maze test showed that acute administration of ASHP and SCH + NKT treatments had higher discrimination index in the object recognition task, more quadrant dwell time and shorter escape latency compared with those in the Morris water maze. The levels of TNF-α, IL-1β and IL-6 were decreased after ASHP and SCH + NKT treatment. The inflammatory response was attenuated by inhibiting TLR4/ NF-κB/ NLRP3 pathway. In addition, ASHP and SCH + NKT treatments significantly restored the activities of superoxide dismutase (SOD), glutathione S-transferase (GST), cyclooxygenase-2 (COX-2), total antioxidant capacity (T-AOC) and inducible nitric oxide syntheses (iNOS), and the levels of glutathione (GSH), malondialdehyde (MDA) and nitric oxide (NO). The histopathological changes of hippocampus were noticeably improved after ASHP and SCH + NKT treatments. These findings demonstrate that ASHP as well as its bioactive components exerted a protective effects on cognitive disorder, inflammatory reaction and oxidative stress.

Keywords Alzheimers' disease · Cognitive dysfunction · Inflammation · Oxidation · Schisandrin · Nootkatone

Introduction

Alzheimer's disease (AD) has become the fourth killer of human health after heart disease, tumor and stroke. It seriously affects the quality of life of the elderly. With the continuous aging of the population, the incidence of AD is increasing (Sosa-Ortiz et al. 2012). The main symptoms of AD are memory impairment, accompanied by an abnormality in personality, cognition, and language (Blennow et al. 2006).

AD has two important pathological features, including the aggregation of extracellular beta amyloid (Aβ) in the forebrain, and the fibrous tangles of tau protein in the cells which lead to the death of neuron cells (Lin and Luo 2011). Inflammation and oxidative stress are closely related to AD. There are new researches find that neuroinflammation can be either the cause of AD or the result of AD (Pimplikar 2014). A large number of proinflammatory cytokines are excessively activated by microglia. The levels of proinflammatory cytokines in cerebrospinal fluid and serum of AD patients increased significantly (Malashenkova et al. 2017). Interleukin-1 (IL-1), Interleukin-6 (IL-6) and tumor necrosis factor (TNF-α) (Rahimifard et al. 2017) are the main factors of leukocyte aggregation into the central nervous system. Toll-like receptors are leading to increased inflammation mediated

✉ Kaishun Bi
kaishunbi.syphu@gmail.com

✉ Ying Jia
jiayingsyphu@126.com

[1] School of Traditional Chinese Materia Medica, Shenyang Pharmaceutical University, Wenhua Road 103, Shenyang 110016, People's Republic of China

[2] School of Functional Food and wine, Shenyang Pharmaceutical University, Wenhua Road 103, Shenyang 110016, People's Republic of China

[3] School of Pharmacy, Shenyang Pharmaceutical University, Wenhua Road 103, Shenyang 110016, People's Republic of China

by increased synthesis of a number of pro-inflammatory cytokines, and Nuclear Factor Kappa B (NF-κB) is shuttled from the cytosol to the nucleus, causing inflammation. Moreover, NACHT, LRR and PYD domains-containing protein 3 inflammasome (NLRP3) is an inflammasome, whose activation is thought to be dependent on NF-κB signaling (Liston and Masters 2017). In recent years, neuroscientists have reached a consensus that the timely treatment of patients with early and mild AD may delay the progression of AD.

In addition, more and more studies have shown that such oxidative damage is directly involved in the pathological process of various neurodegenerative diseases like AD (Phaniendra et al. 2015). Oxidative stress is a pathophysiological state when the free radicals produced by the body exceed the scavenging capacity of their antioxidant system (Butterfield 2018). It is the determinant of Aβ toxicity (Tönnies and Trushina 2017). Aβ can promote the production of oxygen free radicals, and cause mitochondrial dysfunction, then produce oxidative stress, leading to the death of nerve cells (Lee et al. 2006). Superoxide dismutase (SOD) (Contedaban et al. 2018), glutathione peroxidase (GSH-Px) and glutathione S-transferase (GST) (Qu et al. 2016) are critical oxygen free radical clearance enzymes in the body. In addition, glutathione (GSH) is an important antioxidant. Therefore, it is of great significance to comprehend the sources of oxidative stress and the effective antioxidation pathway for understanding the pathogenesis of AD and the development of new treatment methods.

Cyclooxygenase −2 (COX-2) is an important rate limiting enzyme in the biosynthesis of arachidonic acid, prostaglandin and thromboxane A2. It mainly expresses in inflammatory cells and plays an important role in the inflammatory response (Sil and Ghosh 2016a, b). Nitric oxide (NO), as a medium of cell, messenger or cell function regulating factor, participates in many biological activities and pathological processes of the body. It must be generated through the action of nitric oxide syntheses (NOS) in the body. It is found that inducible nitric oxide syntheses (iNOS) can mediate the inflammatory reaction and lead to the pathological process of AD.

There is no drug which could cure AD completely at present, so we pay attention to Traditional Chinese Medicine. Traditional Chinese Medicine has prominent advantages (Miao et al. 2010), such as small side effects, multiple targets and multiple pathways to exert effect. Since ancient time, *Alpinia oxyphylla Miq.* Fructus (AOF) has been used as a traditional Chinese medicine for tonifying kidney and brain. It is widely used in the southern part of China, especially in Hainan province, and people regard it as a condiment in daily life. *Schisandra chinensis* (Turcz.) Baill Fructus (SCF) is a renowned medicine in China. Numerous previous articles have reported that SCF (Di et al. 2012; Song et al. 2015; Xu et al. 2016) and AOF (He et al. 2018; Shi et al. 2015) exhibit the ability of protecting the nervous system. The first combination of these two herbs was in Yizhi Wuwei Pill, which is widely used in Chinese folks to improve memory and it was recorded in the Puji Fang. Hence we based on the Yizhi Wuwei pill to make an herb pair (ASHP) which is composed of SCF and AOF.

Schisandrin (SCH), a quality marker of *Schisandra chinensis* (Turcz.) Baill Fructus recorded in Chinese Pharmacopoeia 2015, has been reported to treat memory loss and dementia (Wei et al. 2018). Nootkatone (NKT) is a compound abundant in *Alpinia oxyphylla Miq.* Fructus. It has been shown to have anti-inflammatory effects and alleviate the symptoms of AD (Wang et al. 2018). However, the biochemical mechanism of SCH and NKT in neuroprotective effect is still dimness. SCH and NKT are the two components with the greatest change in compatibility of ASHP, but it is unclear whether they have synergistic effects in the treatment of AD.

As we have previously reported, ASHP extract had an anti-apoptotic effect to play a neuroprotective role (Qi et al. 2019). However, it is not certain that which components in ASHP worked. The purpose of this study is to detect the changes of compounds' content in ASHP after compatibility and to confirm the neuroprotective components of ASHP.

Materials and methods

Materials

A. oxyphylla and *S. chinensis* were purchased from the TCM shop of Tongrentang Co., Ltd. (Shenyang, China) and identified by Professor Ying Jia (School of Functional Food and wine, Shenyang Pharmaceutical University) according to the guidelines of the Chinese Pharmacopoeia (2015). Subsequently, after intensive mixing AOF and SCF (1:2), 70% ethanol was utilized to extract for 2 h three times by reflux. The ethanol extract was concentrated in a rotary evaporator at 50 °C to obtain the ASHP extract at a yield of 29% (*w/w*, dried extract/crude herb). The residue after vacuum concentration was collected and dissolved in 0.5% sodium carboxymethylcellulose.

Nine authentic compounds were used in this study. The reference compounds protocatechuic acid, chrysin, schisandrin, nootkatone, gomisin A, gomisin B, deoxyschizandrin, schisandrinB and schisandrin C were purchased from Dalian Meilun Biology and Technology Co. Ltd. (Dalian, China). The purities of all reference standards were more than 98% analyzed by HPLC and the chemical structures were shown in Fig. 1.

$A\beta_{1-42}$ peptide was obtained from Sigma-Aldrich (St Louis, MO, USA) and dissolved in physiological saline at a concentration of 1.0 mg/ml. Then it was incubated at 4 °C for 24 h to obtain the oligomeric form. Donepezil was purchased from Dalian Meilun Biology and Technology Co. Ltd.

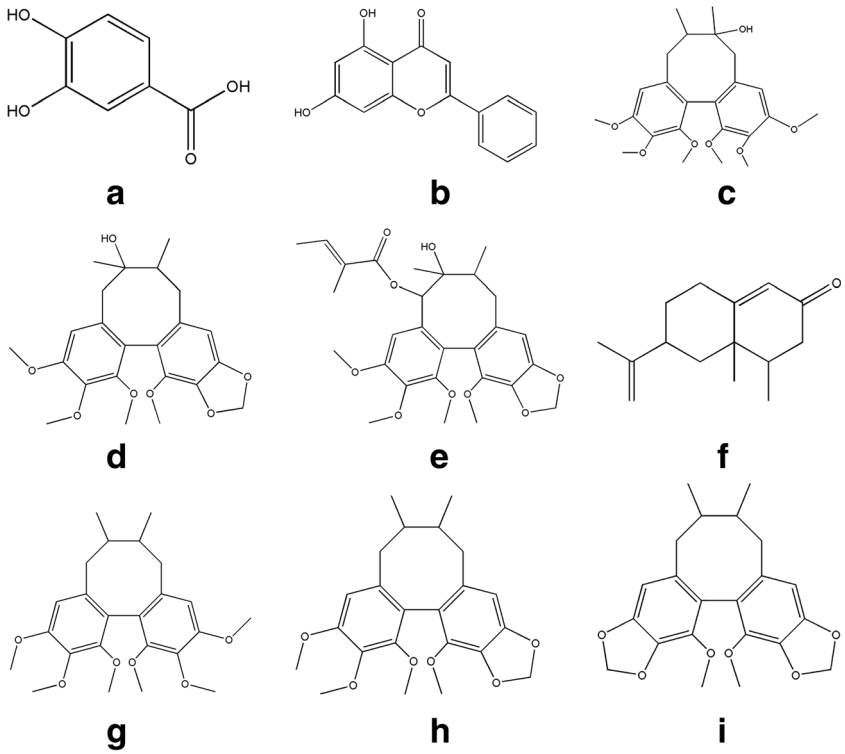

Fig. 1 The chemical structures of 9 reference compounds. **a** Protocatechuic Acid; (**b**) Chrysin; (**c**) Schisandrin; (**d**) Gomisin A; (**e**) Gomisin B; (**f**) Nootkatone; (**g**) Deoxyschizandrin; (**h**) Schisandrin B; (**i**) Schisandrin C

(Dalian, China). Commercial kits used for assay of GSH-Px, GST, GSH, MDA, T-AOC, SOD, NOS and NO were obtained from Jiancheng Institute of Biotechnology (Nanjing, China). ELISA kits used for determination of COX-2, TLR4, NF-κB, NLRP3, TNF-α, IL-1β and IL-6 were purchased from Dalian Meilun Biology and Technology Co. Ltd. (Dalian, China).

Quantitative analysis of 9 components in ASHP

ASHP was qualitatively analyzed employing UPLC method. Samples were eluted on a SBC18 column (2.1 × 100 mm, 1.8 μm). The column and autosampler temperatures were maintained at 30 °C and 4 °C, respectively. The chromatogram was recorded at 254 nm. A mobile phase consisting of water (A) and acetonitrile (B) was applied with the optimized gradient program as follows: 0 ~ 4 min, 2% ~ 10% (B); 4 ~ 5 min, 10 ~ 30% (B); 5 ~ 25 min, 30 ~ 90% (B); 25 ~ 26 min, 90% (B). The flow rate was maintained at 0.3 mL/min, and 2.0 μL of standard and sample solutions were injected in each run.

Animals

All animal procedures were approved by the Animal Ethics Committee of the institution and were in according to the Guidelines for Animal Experimentation of Shenyang Pharmaceutical University. The experiments were performed with male KM mice, weighting 18–22 g were provided by the Central Animal House of Shenyang Pharmaceutical University (Shenyang, China), kept in plastic cages with standard laboratory conditions (temperature 23 ± 2 °C, 12 h: 12 h light/dark cycle, lights on 8 A.M.), had free access to food and water and were allowed to adjust the environment for 7 d before the experiment.

Experimental design

The mice were divided into 7 groups randomly and 8 in each group. Mice were fixed in a stereotaxic instrument after anesthesia according to Tang's method (Tang et al. 2014). The $A\beta_{1-42}$ group and drugs-treated groups were injected with $A\beta_{1-42}$ (3 μl) into the right lateral ventricle of AP, −0.5 mm; ML, −1.1 mm and DV, −3.0 mm within 1 min respect to the brain locator, while the control group were injected with the same amount of saline in the same area. Leave the microsyringe at the injection site for 3 min to facilitate drug diffusion. 3 days recoveries were allowed before successive administration. The control and model groups were intragastric administrationed with distilled water containing 0.5% CMC-Na. The dosage of all groups was 1200 mg/kg of unprocessed Schisandra chinensis, Alpinia oxyphylla or ASHP, which was derived from our preliminary experiment. The ASHP group was treated (i.g.) with 348 mg/kg ethanol extract (1200 mg/kg ASHP × 29% yield), the SCH group was treated (i.g.) with 9.13 mg/kg schisandrin (1200 mg/kg Schisandra chinensis × 0.761%, calculated according to UPLC measured content), the NKT group was treated (i.g.)

with 2.52 mg/kg nootkatone (1200 mg/kg Alpinia oxyphylla × 0.210%, calculated according to UPLC measured content), the SCH + NKT group was treated (i.g.) with 7.84 mg/kg schisandrin +1.64 mg/kg nootkatone (1200 mg/kg ASHP × 0.653% + 1200 mg/kg ASHP × 0.136%, calculated according to UPLC measured content) and the Donepezil group was treated (i.g.) with 0.65 mg/kg donepezil. Behavioral tests were performed after 30 days' administration, and brain biochemical assessment was assessed on the following day.

Behavioral test

Object recognition task

Object Recognition Task experiment consists of three parts: the adaptation period, the familiarity period and the test period (Antunes and Biala 2012). First, Mice were adapted for 10 min. After 30 min interval, mice were allowed to freely explore two same objects for 10 min. The objects were made of plastic. Then, two hours later, the mice were put back in the same box for testing. The two objects were again present, but one object was now replaced by a novel object of the same material but different color and shape. Mice were allowed to explore the environment and objects freely for 5 min, measuring the time it took to explore displaced and non-displaced objects. A discrimination index was used to represent the preference for novel as opposed to familiar object calculated as follows:Discrimination index = (N - F) / (N + F) (N, time spent exploring novel object. F, time spent exploring old object).

Morris water maze test

Morris water maze, a circular water tank 150 cm in diameter and 60 cm high and filled with water of rendered opaque by adding ink at 27 ± 1 °C was carried out to test of spatial learning and memory. As described in previous study (Vorhees and Williams 2006), the tank was divided essentially into 4 quadrants and a platform (8 cm diameter and 10 cm height) was submerged 1 cm below the water surface. Above the tank, a camera was used to record the movements of mice. The test is divided into two phases, namely place navigation test and probe test. The place navigation test was conducted twice daily for five consecutive days, and the mice were tested twice from different points facing the pool wall to start the two trials. The mice were allowed to swim freely to explore the hidden platform within 90 s. If mice succeed in finding the platform during the period and allowed stay on it for 3 s, then the time spent was recorded, but if the mice jumped into the water within 3 s, the track was not terminated until the mice stayed on the platform for 3 s. If the mice failed to find locate the platform within 90 s, then the time was recorded 90 s and the mice were guided to the platform for 20 s. The escape latency was defined as the spent time to reach the platform and the total distance of swimming was record by the camera (BRYAN and DEVAN 1996). 24 h after the last training session, the platform was removed and took out the probe trial. The mice were allowed to look for the removed platform freely for 90 s without inference. In this part, the number of crossing platform and the percentage of time spent in the target quadrant were recorded (D'Hooge and Deyn 2001).

Brain sample collection

After behavioral tests described above, the animals were sacrificed by decapitation and the hippocampi were stripped out quickly, rinsed with physiological saline and quickly frozen in a freezer (−80 °C). Two entire brains in each groups were removed, immersion by 10% formalin solution at 4 °C subsequently until histopathological trial. The brain tissues were weighted, and rapidly homogenized in ice-cold saline (w/v = 1:1) and the homogenates were centrifuged at 3500 rpm at 4 °C for 15 min, the supernatants were transferred to another centrifuge tube for assay.

Biochemical analyses

The supernatant of hippocampus and cerebral cortex tissue obtained was used to measure the levels of anti-inflammatory enzyme activities including TLR4, NF-κB as well as its downstream molecules NLRP3, TNF-α, IL-1β and IL-6; the level of MDA, NO and the activities of SOD, GSH-Px, T-AOC, COX-2, and NOS were detected by assay kits using multifunctional microplate reader.

Hematoxylin-eosin (HE) staining

Hematoxylin-eosin staining is one of the most extensive techniques for observing changes in tissue morphology and the procedure was just as reported in previous report (Ozden et al. 2011). Briefly, the dehydrated sections were stained with hematoxylin solution, washed several times and then stained with eosin solution. Finally, the sections were sealed with a neutral gel for observation.

Immunohistochemical analyses

The sections were obtained as same as 2.8. The Immunohistochemical method we used in this study was as described in Wang's study (Wang et al. 2018). In brief, the sections were incubated overnight with the primary antibody for TLR4 (rabbit IgG, 1:100, Abcam, UK), NF-κB (rabbit IgG, 1:100, Abcam, UK) and NLRP3 (rabbit IgG, 1:100, Abcam, UK) diluted in 5% BSA overnight at 4 °C respectively. Next day, washed slices in PBS three times for 5 min and incubated it with secondary antibody at room temperature for 30 min, then conjugated with horseradish peroxidase, and

detected with 0.025% DAB. Sections were counterstained with hematoxylin and images were taken with an upright microscope Olumpus BX53. Sections were counted manually by two researchers blind to treatments at ×400 magnification.

RNA isolation and quantitative real-time PCR (qPCR)

Total RNA was extracted from the treated tissues using TRIzol reagent from Melone Pharmaceutical Co. (Dalian, China). qPCR was performed with KAPA SYBR FAST qPCR Kit (Kapa biosystems) following the manufacturer's instructions.

In brief, cDNA was prepared using RNA samples (2 μg) to which 1 μg oligo(dT), 0.5 mM deoxynucleotide triphosphate and 200 units of the Revert AidTM H-Minus M-MuLV Reverse Transcriptase enzyme were added. qPCR analysis was performed using primers synthesized, as shown in Tables 1, and 1 μL RT product was incubated with 1 unit Taq DNA polymerase in a 20 μL reaction mixture. Ct values were normalized to β-actin, and the relative gene expression was calculated with the $2^{-\Delta\Delta Ct}$ method.

Statistical analysis

Statistical analyses were performed using GraphPad Prism software 6.0. Data were indicated as mean ± standard deviations. Repeated measures two-way ANOVA followed by post-hoc Tukey's test was performed for the Morris water maze tests of the latency. Other group comparison was performed using one-way ANOVA followed by post-hoc Tukey's test. In all the tests, $p < 0.05$ was considered statistically significant.

Results

UPLC analysis of nine components in ASHP

We quantitatively analyzed nine active components from ASHP. Protocatechuic acid, chrysin and nootkatone were from AOF and protocatechuic acid, schisandrin, gomisin A, gomisin B, deoxyschizandrin, schisandrin B and schisandrin C were from SCF. For the purpose of comparing the content changes of each component in ASHP, which was the compatibility between SCF and AOF in a ratio of 2:1, the theorized content of each compound in ASHP were calculated by the following formula: The theorized content = Content in SCF × proportionality coefficient of SCF in ASHP + Content in AOF × proportionality coefficient of AOF in ASHP (Li et al. 2014). As shown in Fig.2 and Table 2, compared with the theorized content, the contents of protocatechuic acid, gomisin B and deoxyschizandrin were almost unchanged. The contents of schisandrin, gomisin A, nootkatone and showed increments whereas the contents of chrysin, schisandrin B and schisandrin C were decreased after compatibility. Among them, the most dramatic changes in the contents caused by compatibility were schisandrin and nootkatone. The increased rates of schisandrin and nootkatone were 28.8% and 94.3%, respectively (the increased rate = (Content - The theorized content)/ The theorized content). This study provides a strong theoretical basis for our subsequent in vivo experiments.

Effects of ASHP and its main bioactive components on object recognition task

Mice from all seven groups spent the same percent of time exploring both identical objects during the training phase (not shown). The data revealed that model group mice spent less time exploring the novel object compared to the familiar object ($p < 0.001$; Fig. 3) indicating that they did not remember the familiar object from the object familiarization phase and thus had a preference for the familiar object. In contrast, mice from the ASHP group ($p < 0.001$; Fig. 3), SCH + NKT group ($p < 0.01$; Fig. 3) and donepezil group ($p < 0.001$; Fig. 3) spent more time exploring the novel object suggesting that these rats remembered the novel object.

Table 1 Primer sequences used for qPCR analysis

Gene	Forward	Reverse
TLR4	5′-TCAGAGCCGTTGGTGTATCTT-3′	5′-CCTCAGCAGGGACTTCTCAA-3′
NF-κB	5′-GATAGCCCTTGCATCCTTAC-3′	5′-GCTGCCTTTGGTCTTTCTCG-3′
NLRP3	5′-AGAAGCTGGGGTTGGTGAATT-3′	5′-GTTGTCTAACTCCAGCATCTG-3′
TNF-α	5′- TTGACCTCAGCGCTGAGTTG - 3′	5′- CCTGTAGCCCACGTCGTAGC - 3′
IL-1β	5’-GGAACCCGTGTCTTCCTAAAG-3′	5’-CTGACTTGGCAGAGGACAAAG-3′
IL-6	5′- CACTTCACAAGTCGGAGGCT- 3′	5′- TCTGACAGTGCATCATCGCT- 3′
β-actin	5′-CTGTGCCCATCTACGAGGGCTAT-3′	5′-TTTGATGTCACGCACGATTTCC-3′

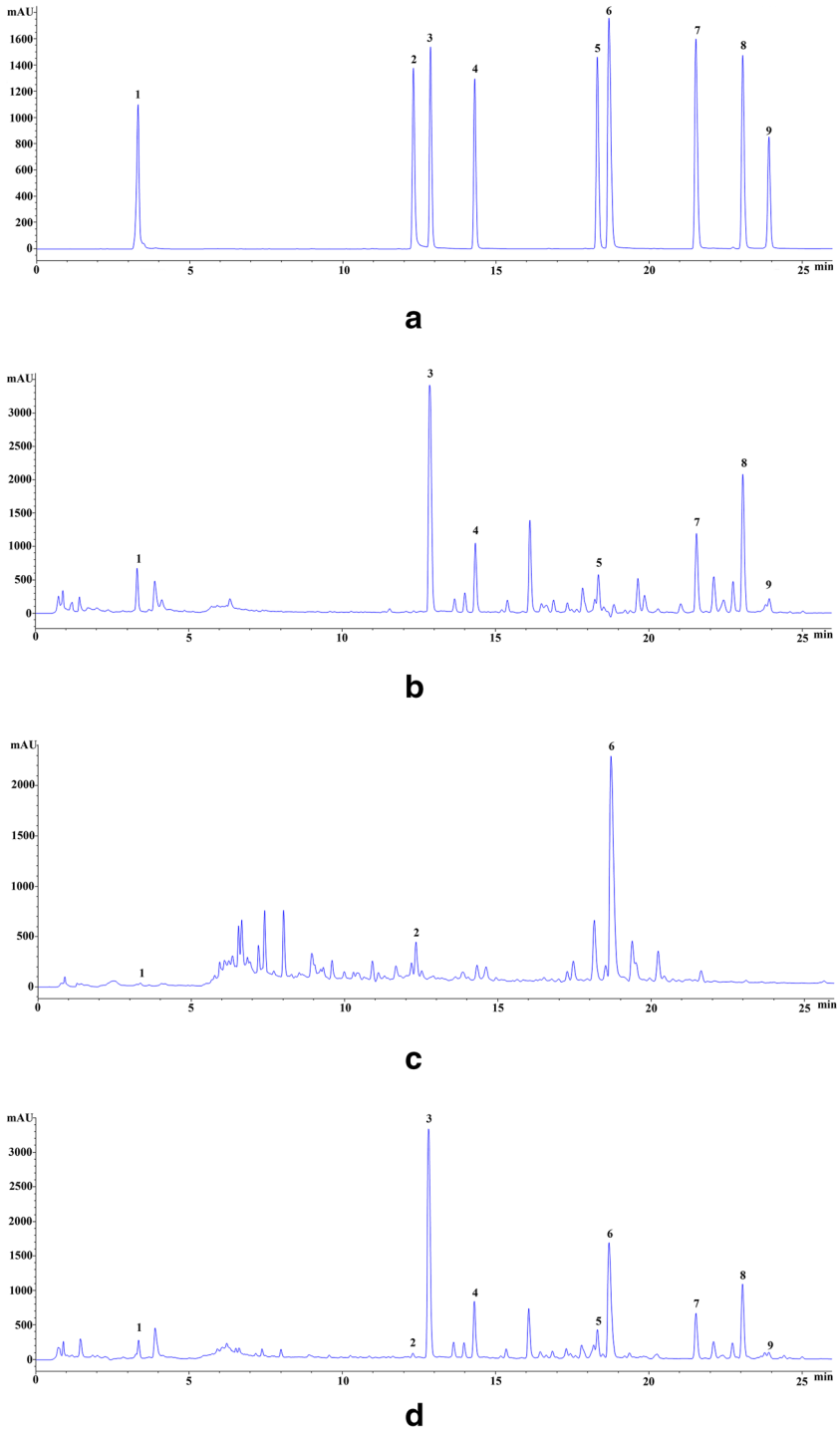

Fig. 2 UPLC chromatograms at 254 nm. Chromatograms: (**a**) mixed reference substance; (**b**) SCF extract; (**c**) AOF extract; (**d**) ASHP extract. Peak: 1. Protocatechuic Acid; 2. Chrysin; 3. Schisandrin; 4. Gomisin A; 5. Gomisin B; 6. Nootkatone; 7. Deoxyschizandrin; 8. Schisandrin B; 9. Schisandrin C

Effects of ASHP and its main bioactive components on Morris water maze test

During the orientation navigation experiment, there was no significant difference in the latency among all the groups in the first 2 days. From the third day, the model group took longer time to reach the platform compared with the control group ($p < 0.01$, Fig. 4a). ASHP, SCH + NKT and donepezil treatments all significantly ameliorated the effect of $A\beta_{1-42}$ on escape latency. During the subsequent spatial probe test, there is no significant difference in speed among groups (Fig. 4b). Moreover, the mice in control, ASHP, SCH + NKT and donepezil groups spent much more time in the target quadrant in varying degree. It is worth noting that after the combination of SCH and NKT ($p < 0.01$, Fig. 4c), the quadrant dwell time percentage is significantly longer than their individual use.

Table 2 The main bioactive components contents in SCF, AOF and ASHP extracts

Group	SCF (mg/g)	AOF (mg/g)	ASHP (mg/g)	Theorized content (mg/g)
protocatechuic acid	0.21	0.06	0.15	0.16
chrysin	–	0.18	0.04	0.06
Schisandrin	7.61	–	6.53	5.07
Gomisin A	2.60	–	2.17	1.73
Gomisin B	2.02	–	1.36	1.35
Nootkatone	–	2.10	1.36	0.70
Deoxyschizandrin	2.90	–	1.94	1.93
Schisandrin B	5.69	–	3.72	3.79
Schisandrin C	0.64	–	0.28	0.42

Results of histological examinations

The neurons of the vehicle group in the CA1 region have shown a marked changing and a distinct difference in neuronal structure. Aβ induced nuclear rarefaction, disordered, pronounced shrinkage nuclei and swollen neuronal bodies in the CA1 region. The ASHP and SCH + NKT treatments significantly inhibited the histopathological damage, as those pictures shown the nucleoli were clearly visible, and there was no edema cell (Fig. 5).

Effect of ASHP and its main bioactive components on the level of TLR4, NF-κB, and NLRP3 in hippocampus

In order to elucidate the anti-inflammatory effects of ASHP in brain tissue, the anti-inflammatory enzymes levels including TLR4, NF-κB, and NLRP3 were determined. As shown in Fig.6a-c, compared with control group, the injection of $A\beta_{1-42}$ could significantly increase the levels of TLR4, NF-κB and NLRP3. Meanwhile, ASHP and SCH + NKT treatments could dramatically downregulate the anti-inflammatory enzymes. However, SCH and NKT alone groups did not exhibit the same anti-inflammatory activity. The expressions of TLR4, NF-κB, and NLRP3 in hippocampus were further detected by immunohistochemistry. Consistent with the ELISA assay results, the expressions of TLR4, NF-κB, and NLRP3 of the control group were less, while the expressions of TLR4, NF-κB, and NLRP3 in model group were significantly increased. The expressions of TLR4, NF-κB, and NLRP3 in hippocampus of ASHP and SCH + NKT groups were significantly decreased (Fig. 4d-f).

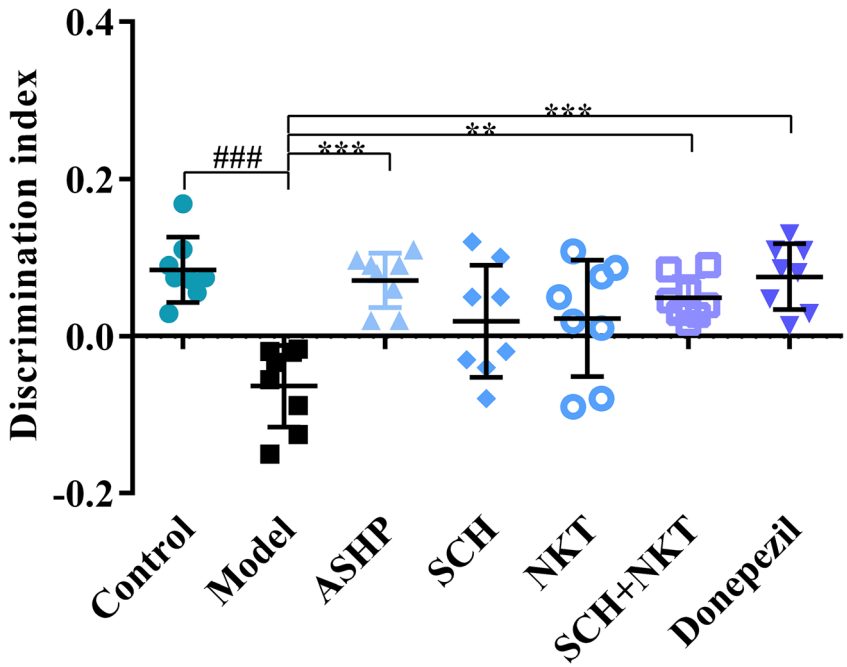

Fig. 3 Effects of the bioactive components in ASHP on Discrimination index (**a**) in the object recognition task. The values represent the mean ± SD ($n = 8$ in each group), $^{***}p < 0.001$ versus the model group; $^{###}p < 0.001$ versus the control group

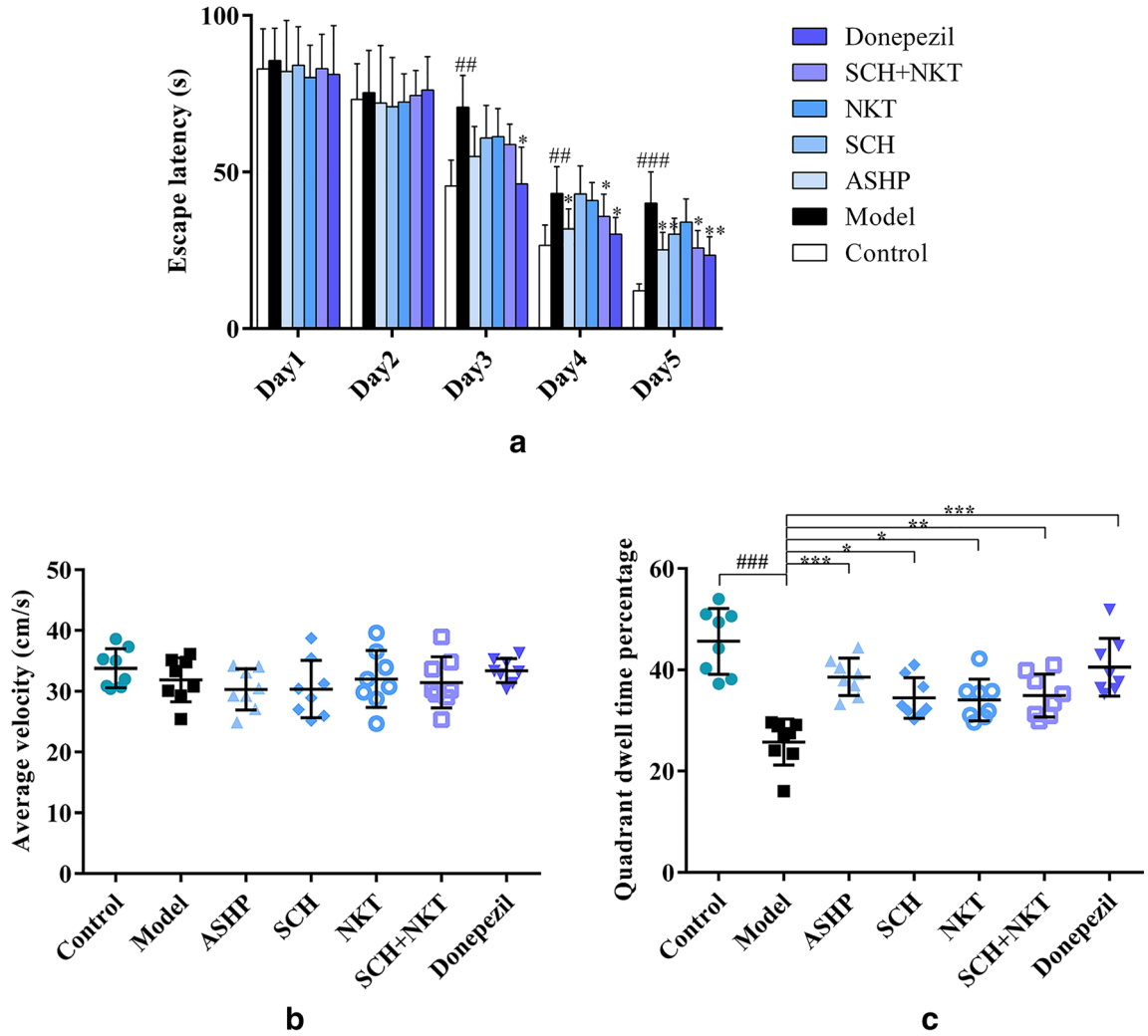

Fig. 4 Effects of the bioactive components in ASHP on Escape latency (**a**), The average velocity of mice (**b**) and Quadrant dwell time percentage (**c**) in the Morris water maze test. The values represent the mean ± SD ($n = 8$ in each group), $^{*}p < 0.05$, $^{**}p < 0.01$ and $^{***}p < 0.001$ versus the model group; $^{###}p < 0.001$ versus the control group

Based on the above results, we further use the qPCR analysis to detect the mRNA levels of TLR4, NF-κB, and NLRP3. The results showed that expressions of TLR4, NF-κB, and NLRP3 were altered at mRNA levels in mice given Aβ treated, while ASHP and SCH + NKT groups reduced this alternation (Fig. 6 G-I).

Effect of ASHP and its main bioactive components on the level of TNF-α, IL-1β, IL-6 in hippocampus

Moreover, we detected the levels of inflammatory factors including TNF-α, IL-1β and IL-6. As shown in Fig.7, compared with control group, the model group could significantly increase the levels of TNF-α, IL-1β, IL-6 ($p < 0.001$, Fig. 7a-c). ASHP and SCH + NKT treatments could significantly downregulate the anti-inflammatory enzymes in the hippocampus of drug treated mice compared to the model group (Fig. 7a-c).

A qPCR analysis was also established to detect the change of mRNA levels. As shown in Fig. 7d-e, The mRNA levels of TNF-α, IL-1β, IL-6 in model group increased significantly ($p < 0.001$). However, the single administration of NKT or SCH had no effect on the mRNA levels of these three inflammatory factors. The ASHP and SCH + NKT groups significantly reduced the mRNA levels of inflammatory factors ($p < 0.001$).

Effect of ASHP and its main bioactive components on the activities of T-AOC, SOD, GSH-Px, GST as well as the level of MDA and GSH

We evaluated the activities or levels of T-AOC, MDA, SOD, GSH-Px, GST and GSH to elucidate whether $A\beta_{1-42}$ administration makes any change in the antioxidant status within the brain or this change is reversible by the treatment of ASHP. Compared with the control group, the model group generated

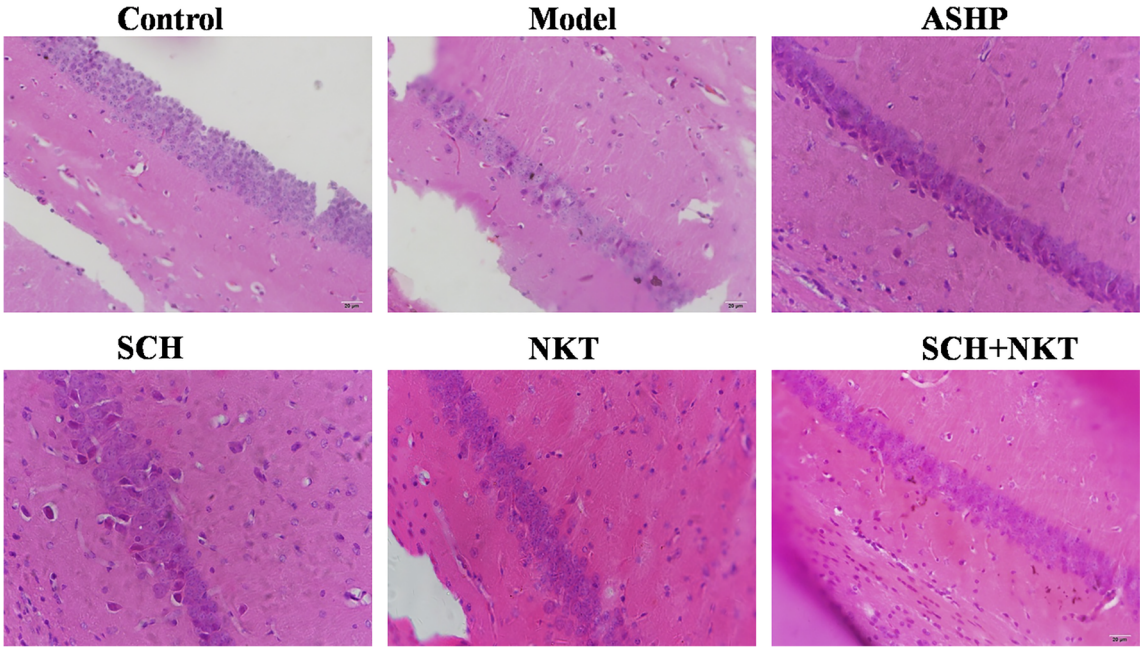

Fig. 5 Effects of the bioactive components in ASHP on the morphology and the number of neurons in an $A\beta_{1-42}$- induced AD mouse model. Light micrographs of hippocampal neurons from the CA1 region

a dramatic decrease in the activities of SOD and T-AOC as well as a significant increase in MDA level (Table 3). ASHP and SCH + NKT treatments significantly restored the level of SOD ($p < 0.001$ and $p < 0.01$, respectively) and decreased the level of MDA ($p < 0.001$ and $p < 0.01$, respectively) and T-AOC ($p < 0.001$ and $p < 0.001$, respectively). As shown in Table 4, ASHP and SCH + NKT treatments increased the activity of GST ($p < 0.01$ and $p < 0.05$, respectively) and the level of GSH ($p < 0.01$ and $p < 0.01$, respectively) while decreased the activity of GSH-Px ($p < 0.001$ and $p < 0.01$, respectively).

Effect of ASHP and its main bioactive components on the level of COX-2, iNOS, NO

Next we detected the activities of COX-2 and iNOS, and the level of NO. As shown in Table 5, compared with the control group, the activities of COX-2 and iNOS, and the level of NO increased significantly in the model group. ASHP and SCH + NKT treatments significantly decreased the activities of COX-2 ($p < 0.01$, $p < 0.01$, respectively), iNOS ($p < 0.05$) and the level of NO ($p < 0.01$, $p < 0.05$, respectively).

Discussion

Schisandra chinensis and Alpinia oxyphylla are the most important components of 'yizhiwuweiwan', and ASHP is the result of simplifying 'yizhiwuweiwan'. After the compatibility of herbs, its constituents have changed to some extent (Wang et al. 2012). In this study, we quantitatively analyzed 9 bioactive components in ASHP and compared them with those in single herb. The increased rates of NKT and SCH reached 94.3% and 28.8%, respectively, which were the two components that increased most after compatibility. That is why we next focus on the in vivo activity studies of NKT and SCH.

Progressive neuronal loss is one of the typical pathological changes of AD and neuronal apoptosis plays an important role in the pathogenesis of AD. The overexpression of inflammatory factors in the brain not only enlarges the area of the senile plaque but also promotes the increase of the deposition of β-amyloid, which reduces the ability of the brain to swallow and remove Aβ, and causes the loss of neurons (Liao et al. 2016). TLR4 is a lipopolysaccharide receptor that plays a vital role in innate immune responses (Sha et al. 2011). Recent studies have implicated the significant effect of TLR4 in neurodegeneration and disease progression in AD patients (Zhang et al. 2013). NF-κB can enhance the gene transcription of TNF-a, IL-1, IL-6 and IL-8, mainly by binding to the κB site of the promoter sites of the genes (Shi et al. 2016). Moreover, the important role of NF-κB factors in the central nervous system through toll-like receptor activation has been well established. The NF-κB signaling pathway can be activated and the processing and secretion of IL-1β are promoted at the same time. In our study, we first

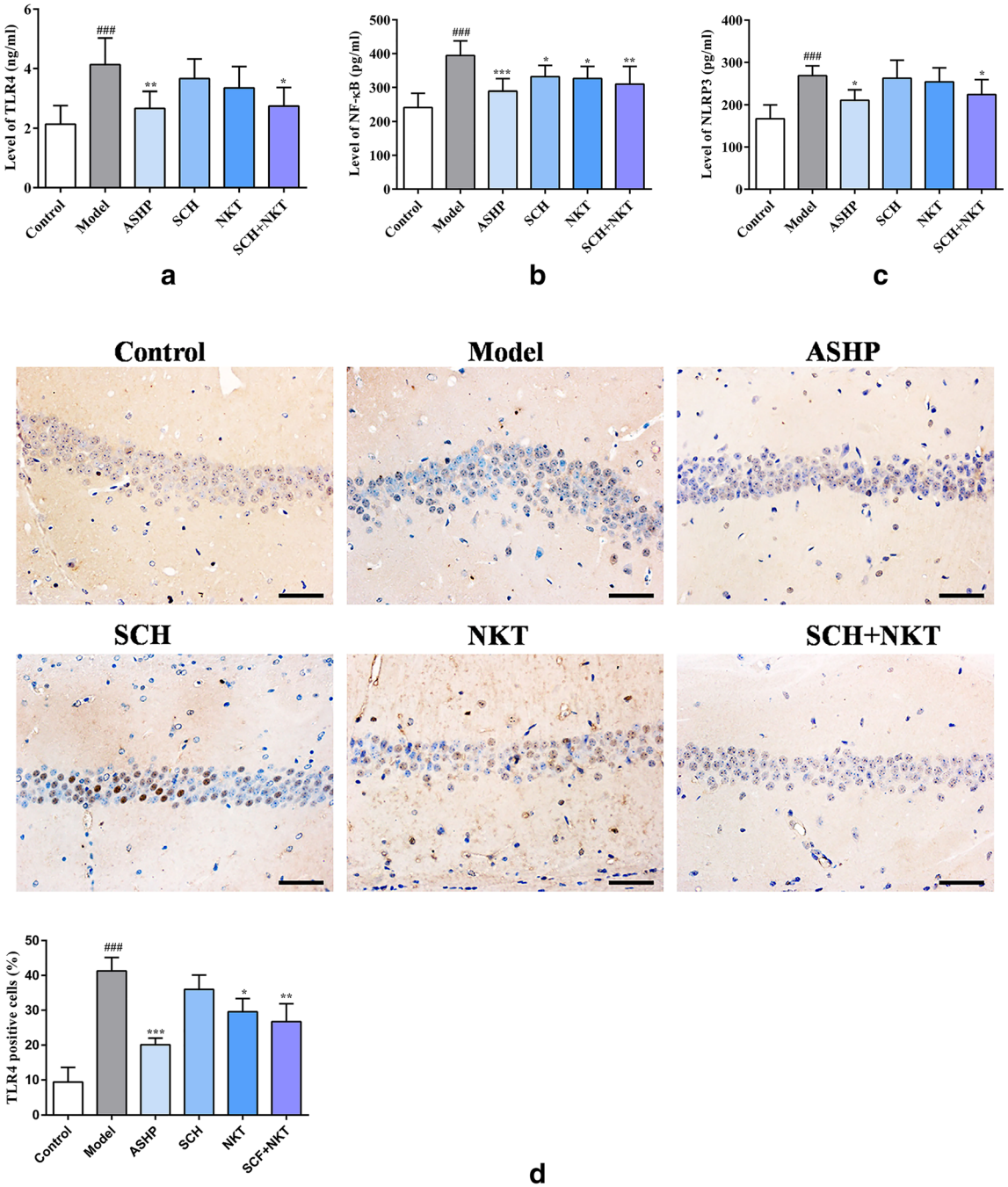

Fig. 6 Effects of the bioactive components in ASHP on the levels of TLR4, NF-κB and NLRP3 in the hippocampus (**a**, **b** and **c**) detected by ELISA assay. The expressions of TLR4, NF-κB and NLRP3 were detected by immunohistochemistry. Scale bar: 50 μm. The magnification was 400×. The levels of TLR4, NF-κB and NLRP3 in the hippocampus (**d**, **e** and **f**) detected by ELISA assay. The mRNA levels of TLR4, NF-κB and NLRP3 in the hippocampus (**g**, **h** and **i**). The values represent the mean ± SD ($n = 3$ in each group), $^{**}p < 0.01$, $^{***}p < 0.001$ versus the model group; $^{###}p < 0.001$ versus the control group

detected the levels of TLR4, NF-κB and NLRP3 using ELISA assay and immunohistochemistry. Then qPCR technique was used to examine their mRNA levels. The results showed that ASHP treatment could inhibit the TLR4/ NF-κB/ NLRP3 pathway and decrease inflammatory factors in the brain.

AD is a degenerative disease of the nervous system. Cellular aging is one of the most dangerous factors, and the pathogenesis of AD is closely related to the damage of free radicals (Dubinina and Pustygina 2007; Sohal 2002). According to the theory of free radical injury, neural tissue is more vulnerable to

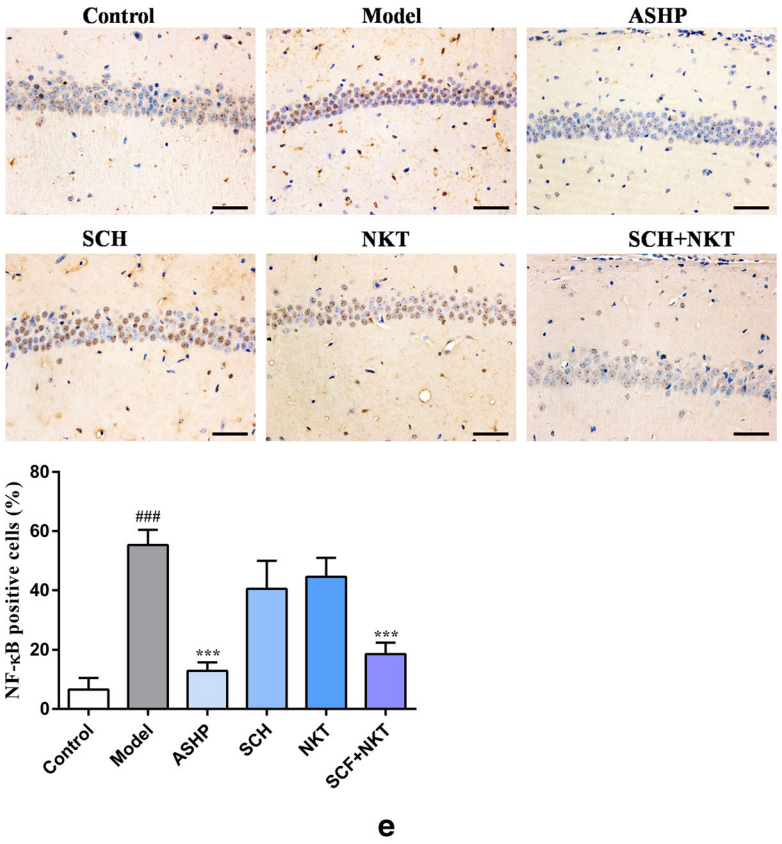

e

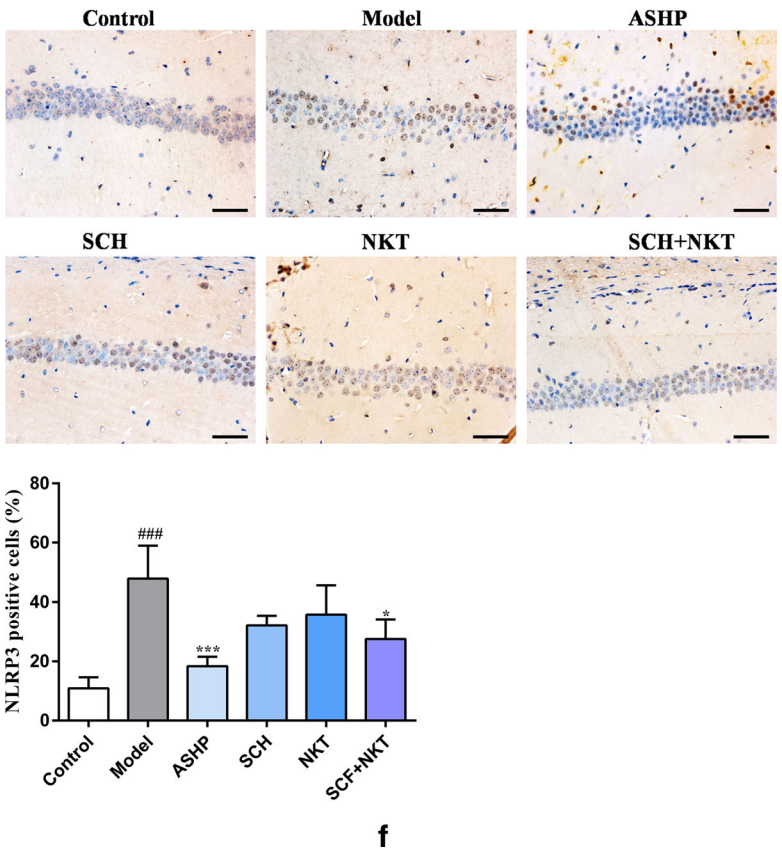

f

Fig. 6 (continued)

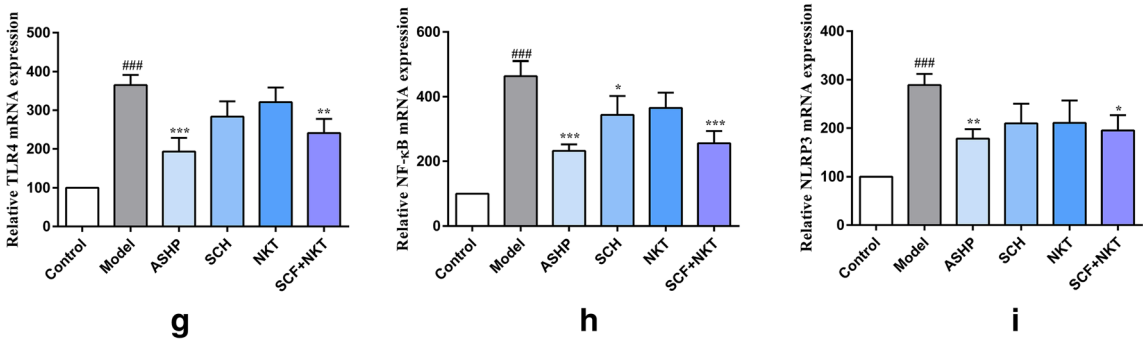

Fig. 6 (continued)

oxygen free radicals because of its different structure from other tissues (Halliwell 2001; Shi and Gibson 2007). In cell metabolism, a large number of free radicals will damage DNA and other macromolecules, accelerating cell death and causing degenerative diseases, which can lead to the aging. Free radicals have oxygen free radicals and hydroxyl radicals. SOD is an important antioxidant enzyme in the body and it can remove free radicals and prevent the free radical chain reaction initiated by O2 (Manczak et al. 2006; Richardson 2010). In addition, the newly formed unsaturated fatty acid radical is combined with the unsaturated fatty acid of another molecule to produce a new molecule of lipid free radical, which is decomposed into MDA (Gustaw-Rothenberg et al. 2010). Therefore, the degree of lipid peroxidation damage can be marked by MDA level.

In this study, the antioxidant enzyme activities in the brain of mice were detected. Our data showed that ASHP as well as its bioactive components remarkably improved the activity of SOD, T-AOC, whilst significantly reduced the level of MDA. On the other hand, GSH-Px and GST work together with GSH in the decomposition of hydrogen peroxide or other organic hydroperoxides. ASHP as well as its bioactive components increased the activity of GST and the level of GSH, while the activity of GSH-Px in ASHP and SCH + NKT groups was lower than that in the model

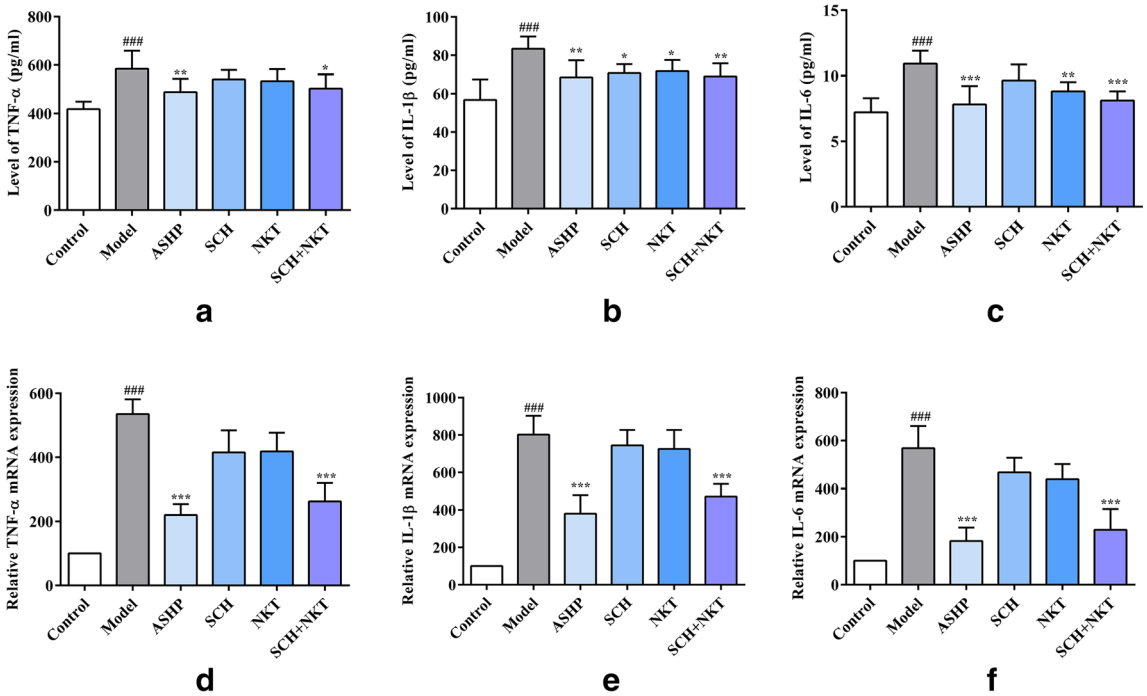

Fig. 7 Effects of the bioactive components in ASHP on TNF-α (**a**), IL-1β (**b**) and IL-6 (**c**) levels and the mRNA levels of TNF-α (**d**), IL-1β (**e**) and IL-6 (**f**) in the hippocampus. The values represent the mean ± SD ($n = 3$ in each group), $^{**}p < 0.01$, $^{***}p < 0.001$ versus the model group; $^{###}p < 0.001$ versus the control group

Table 4 Effects of the bioactive components in ASHP on the activities of GSH-px and GST, and the level of GSH

Group	GSH-Px (U/mgprot)	GST (U/mgprot)	GSH (μmol/gprot)
Control	123.37 ± 18.21	65.13 ± 5.87	136.66 ± 9.29
Model	185.02 ± 29.39$^{\#\#\#}$	36.93 ± 8.59$^{\#\#}$	74.67 ± 9.07$^{\#\#\#}$
ASHP	137.42 ± 20.96***	60.63 ± 6.23**	115.02 ± 12.29**
SCH	150.75 ± 5.75*	54.87 ± 6.55*	103.00 ± 9.54*
NKT	161.40 ± 7.07	49.37 ± 9.44	80.33 ± 7.51
SCH + NKT	141.19 ± 9.01**	57.87 ± 4.73*	108.14 ± 7.32**

Data were shown as mean ± SD ($n = 3$ in each group). $^{*}p < 0.05$, $^{**}p < 0.01$ and $^{***}p < 0.001$ versus the model group; $^{\#\#\#}p < 0.001$ versus the control group

group. We speculated that the addition of GSH-Px activity in model group may merely be a manifest of an antioxidant response to the increased peroxidative stress induced by Aβ. Our result was consistent with (Nuray et al. 2003). Therefore, we believed that ASHP as well as its bioactive components inhibited oxidative stress mainly by increasing GST activity and GSH level. Based on the effects of ASHP as well as its bioactive components on inflammatory markers and oxidative stress indicators, we conjectured that the anti-inflammatory mechanism of ASHP as well as its bioactive components interrupts oxidative stress through the antioxidant stress pathway, mainly by promoting the metabolism of arachidonic acid and reducing the release of various inflammatory mediators. Hence we next tested the activities of COX-2 and iNOS as well as the level of NO. Inflammation, a complex network of molecular signaling pathways, is a complex process mediated by a variety of molecular mechanisms, including the two important molecular mechanisms, iNOS (Youn et al. 2007) and COX-2. The two inducible synthases have the same regulation mechanism and the main inflammatory signal transduction pathway (Sakthivel and Guruvayoorappan 2015). ASHP as well as its bioactive components can suppress the expression of target gene and protein of NOS by inhibiting the NF-κB signal transduction of in the MAPK signal transduction pathway, control the amount of NO generation and oxidative stress, and maintain the normal physiological level of NO and enzyme activity. ASHP as well as its bioactive components inhibits the expression of COX-2 and further downregulated the biosynthesis of prostaglandin E2, which can inhibit the expression of inflammatory cytokines, increase the expression of anti-inflammatory mediators, block the vicious circulation pathway, and play an anti-inflammatory effect. Compared to the control group, the activities of COX-2, and iNOS as well as the level of NO in the hippocampus and cerebral cortex of the model mice increased significantly, and the activities or level of the three indexes decreased significantly after ASHP as well as its bioactive components treatments in the hippocampus (Eslami et al. 2017). The results showed that COX-2 and iNOS may play an important role in the pathogenesis of AD.

Based on the above findings, we hypothesized that the anti-inflammatory mechanism of ASHP as well as its bioactive components is to interrupt oxidative stress through promoting the metabolism of arachidonic acid and accumulating the phagocytic cells in inflammatory foci under the action of inflammatory factors.

Table 3 Effects of the bioactive components in ASHP on the activities of SOD, GSH-px and T-AOC, and the level of MDA

Group	SOD (U/mgprot)	T-AOC (U/mgprot)	MDA (nmol/mgprot)
Control	49.15 ± 6.78	2.71 ± 0.23	5.25 ± 0.91
Model	23.98 ± 6.07$^{\#\#\#}$	1.87 ± 0.40$^{\#\#}$	9.74 ± 0.90$^{\#\#\#}$
ASHP	39.64 ± 6.43***	2.63 ± 0.43**	7.04 ± 0.92***
SCH	34.11 ± 5.15*	2.56 ± 0.22*	8.01 ± 0.93*
NKT	28.04 ± 4.59	2.46 ± 0.30*	7.94 ± 0.59*
SCH + NKT	37.27 ± 4.41**	2.62 ± 0.36**	7.61 ± 0.86**

Data were shown as mean ± SD ($n = 3$ in each group). $^{*}p < 0.05$ and $^{**}p < 0.01$ versus the model group; $^{\#\#\#}p < 0.001$ versus the control group

Table 5 Effects of the bioactive components in ASHP on the activities of COX-2 and iNOS, and the level of NO.

Group	COX-2 (U/gprot)	iNOS (U/mgprot)	NO (μmol/mgprot)
Control	412.67 ± 27.08	1.17 ± 0.08	2.15 ± 0.38
Model	631.8 ± 102.91$^{\#\#}$	2.01 ± 0.39$^{\#\#\#}$	3.24 ± 0.53$^{\#\#}$
ASHP	422.13 ± 22.08**	1.59 ± 0.22*	2.29 ± 0.18**
SCH	456.11 ± 44.65*	1.707 ± 0.10	3.09 ± 0.22
NKT	461.3 ± 35.35*	1.69 ± 0.07	3.01 ± 1.03
SCH + NKT	434.37 ± 52.61**	1.64 ± 0.11*	2.41 ± 0.29*

Data were shown as mean ± SD ($n = 3$ in each group). $^{*}p < 0.05$, $^{**}p < 0.01$ and $^{***}p < 0.001$ versus the model group; $^{\#\#}p < 0.01$ and $^{\#\#\#}p < 0.001$ versus the control group

Conclusion

The present study demonstrated that ASHP as well as its bioactive components potentially reversed alterations in cognitive behavioral, biochemical and histopathological changes induced by $A\beta_{1-42}$ in vivo. These impactful effects of ASHP as well as its bioactive components might be attributed by cutting down the damage of oxidative stress, inhibiting the TLR4/ NF-κB/ NLRP3 inflammatory signaling pathways. Our findings suggested that ASHP as well as its bioactive components might be a potential therapy in the treatment of cognitive and behavioral deficits.

Acknowledgements This study was supported by the National Natural Science Foundation of China (no. 81573580). Key laboratory of polysaccharide bioactivity evaluation of TCM of Liaoning Province. Key techniques study of consistency evaluation of drug quality and therapeutic effect (18-400-4-08) and Liaoning Distinguished Professor Project for Ying Jia (2017).

Compliance with ethical standards

Conflict of interest The authors have no conflict of interest to declare.

References

Antunes M, Biala G (2012) The novel object recognition memory: neurobiology, test procedure, and its modifications. Cogn Process 13: 93–110

Blennow K, Leon MJD, Zetterberg H (2006) Alzheimer's disease. Lancet 368:387–403

BRYAN D, DEVAN EHG (1996) Dissociation of hippocampal and striatal contributions to spatial navigation in the water maze. Neurobiol Learn Mem 66

Butterfield, D.A., 2018. Perspectives on oxidative stress in Alzheimer's disease and predictions of future research emphases. Journal of Alzheimers Disease 1–11

Contedaban A, Ambike V, Régis Guillot, et al., (2018) A metallo prodrug to target cu(II) in the context of Alzheimer's disease. Chemistry 24:5095–5099

D'Hooge R, Deyn PPD (2001) Applications of the Morris water maze in the study of learning and memory. Brain Res Rev 36:60–90

Di, H., et al., 2012. Schizandrin, an Antioxidant Lignan from Schisandra chinensis, Ameliorates Aβ1–42-Induced Memory Impairment in Mice. Oxidative Medicine and Cellular Longevity,2012,(2012-5-22). 2012**,** 721721

Dubinina EE, Pustygina AV (2007) Free radical processes in aging, neurodegenerative diseases and other pathological states. Biochemistry Supplement 1:284–298

Eslami SM, Ghasemi M, Bahremand T, Momeny M, Gholami M, Sharifzadeh M, Dehpour AR (2017) Involvement of nitrergic system in anticonvulsant effect of zolpidem in lithium-pilocarpine induced status epilepticus: evaluation of iNOS and COX-2 genes expression. Eur J Pharmacol 815:454–461

Gustaw-Rothenberg KA, Lerner A, Perry G, Siedlak SL, Zhu X, Smith MA (2010) MDA and GSH levels in newly diagnosed Alzheimer's disease patients: a population-based study. Alzheimers & Dementia the Journal of the Alzheimers Association 6:S510–S511

Halliwell B (2001) Role of free radicals in the neurodegenerative diseases. Drugs Aging 18:685–716

He B, Xu F, Xiao F, Yan T, Wu B, Bi K, Jia Y (2018) Neuroprotective effects of nootkatone from Alpiniae oxyphyllae Fructus against amyloid-β-induced cognitive impairment. Metab Brain Dis 33: 251–259

Lee HG et al (2006) Amyloid-beta toxicity in Alzheimer disease: the null versus the alternate hypotheses. In: Biennial Meeting of the Asian-Pacific-Society-For-Neurochemistry, pp 12–12

Li W, Tang Y, Qian Y, Shang E, Wang L, Zhang L, Su S, Duan JA (2014) Comparative analysis of main aromatic acids and phthalides in Angelicae Sinensis Radix, chuanxiong Rhizoma, and Fo-Shou-san by a validated UHPLC-TQ-MS/MS. J Pharm Biomed Anal 99:45–50

Liao Y, Qi XL, Cao Y, Yu WF, Ravid R, Winblad B, Pei JJ, Guan ZZ (2016) Elevations in the levels of NF-κB and inflammatory chemotactic factors in the brains with Alzheimer's disease - one mechanism may involve α3 nicotinic acetylcholine receptor. Curr Alzheimer Res 13:1290–1301

Lin LF, Luo HM (2011) Screening of treatment targets for Alzheimer's disease from the molecular mechanisms of impairment by β-amyloid aggregation and tau hyperphosphorylation. Neurosci Bull 27:53–60

Liston A, Masters SL (2017) Homeostasis-altering molecular processes as mechanisms of inflammasome activation. Nat Rev Immunol 17: 208–214

Malashenkova IK, Khailov NA, Krynskii SA, Ogurtsov DP, Kazanova GV, Velichkovskii BB, Selezneva ND, Fedorova YB, Ponomareva EV, Kolykhalov IV, Gavrilova SI, Didkovskii NA (2017) Levels of proinflammatory cytokines and vascular endothelial growth factor in patients with Alzheimer's disease and mild cognitive impairment. Neurosci Behav Physiol 47:694–698

Manczak M, Anekonda TS, Henson E, Park BS, Quinn J, Reddy PH (2006) Mitochondria are a direct site of Aβ accumulation in Alzheimer's disease neurons: implications for free radical generation and oxidative damage in disease progression. Hum Mol Genet 15: 1437–1449

Miao J et al (2010) Clinical studies with traditional Chinese medicine in the past decade and future research and development. Planta Med 76:2048

Nuray N, Ulusu MS, Avci A, Canbolat O, Ozansoy G, Ari N, Bali M, Stefek M, Stolc S, Gajdosik A, Karasu Ç (2003) Pentose phosphate pathway, glutathione-dependent enzymes and antioxidant defense during oxidative stress in diabetic rodent brain and peripheral organs: effects of Stobadine and vitamin E. Neurochem Res 28: 815–823

Ozden H, Durmaz R, Kanbak G, Uzuner K, Aral E, Kartkaya K, Kabay SC, Atasoy MA (2011) Erythropoietin prevents nitric oxide and cathepsin-mediated neuronal death in focal brain ischemia. Brain Res 1370:185–193

Phaniendra A, Jestadi DB, Periyasamy L (2015) Free radicals: properties, sources, targets, and their implication in various diseases. Indian J Clin Biochem 30:11–26

Pimplikar SW (2014) Neuroinflammation in Alzheimer's disease: from pathogenesis to a therapeutic target. J Clin Immunol 34(Suppl 1): S64

Qi Y, Cheng X, Jing H, Yan T, Xiao F, Wu B, Bi K, Jia Y (2019) Effect of Alpinia oxyphylla-Schisandra chinensis herb pair on inflammation and apoptosis in Alzheimer's disease mice model. J Ethnopharmacol 237:28–38

Qu M-H, Yang X, Wang Y, Tang Q, Han H, Wang J, Wang GD, Xue C, Gao Z (2016) Docosahexaenoic acid-phosphatidylcholine improves cognitive deficits in an Aβ23-35-induced Alzheimer's disease rat model. Curr Top Med Chem 16:558–564

Rahimifard M, Maqbool F, Moeini-Nodeh S, Niaz K, Abdollahi M, Braidy N, Nabavi SM, Nabavi SF (2017) Targeting the TLR4 signaling pathway by polyphenols: a novel therapeutic strategy for neuroinflammation. Ageing Res Rev 36:11–19

Richardson JS (2010) Free radicals in the genesis of Alzheimer's disease. Ann N Y Acad Sci 695:73–76

Sakthivel KM, Guruvayoorappan C (2015) Acacia ferruginea inhibits inflammation by regulating inflammatory iNOS and COX-2. J Immunotoxicol 13:127–135

Sha T, Iizawa Y, Ii M (2011) Combination of imipenem and TAK-242, a toll-like receptor 4 signal transduction inhibitor, improves survival in a murine model of polymicrobial sepsis. Shock. 35:205–209

Shi Q, Gibson GE (2007) Oxidative stress and transcriptional regulation in Alzheimer disease. Alzheimer Dis Assoc Disord 21:276–291

Shi SH, Zhao X, Liu AJ, Liu B, Li H, Wu B, Bi KS, Jia Y (2015) Protective effect of n-butanol extract from Alpinia oxyphylla on learning and memory impairments. Physiol Behav 139:13–20

Shi ZM, Han YW, Han XH, Zhang K, Chang YN, Hu ZM, Qi HX, Ting C, Zhen Z, Hong W (2016) Upstream regulators and downstream effectors of NF-kappaB in Alzheimer's disease. J Neurol Sci 366: 127–134

Sil S, Ghosh T (2016a) Role of cox-2 mediated neuroinflammation on the neurodegeneration and cognitive impairments in colchicine induced rat model of Alzheimer's disease. J Neuroimmunol 291:115–124

Sil S, Ghosh T (2016b) Cox-2 plays a vital role in the impaired anxiety like behavior in colchicine induced rat model of Alzheimer disease. Behav Neurol 2016:1501527

Sohal RS (2002) Role of oxidative stress and protein oxidation in the aging process. Free Radic Biol Med 33:37–44

Song JX et al (2015) Protective effects of dibenzocyclooctadiene lignans from Schisandra chinensis against beta-amyloid and homocysteine neurotoxicity in PC12 cells. Phytother Res 25:435–443

Sosa-Ortiz AL, Acosta-Castillo I, Prince MJ (2012) Epidemiology of dementias and Alzheimer's disease. Arch Med Res 43:600–608

Tang SS, Hong H, Chen L, Mei ZL, Ji MJ, Xiang GQ, Li N, Ji H (2014) Involvement of cysteinyl leukotriene receptor 1 in Aβ1–42-induced neurotoxicity in vitro and in vivo. Neurobiol Aging 35:590–599

Tönnies E, Trushina E (2017) Oxidative stress, synaptic dysfunction, and Alzheimer's disease. Journal of Alzheimers Disease Jad. 57:1105–1121

Vorhees CV, Williams MT (2006) Morris water maze: procedures for assessing spatial and related forms of learning and memory. Nat Protoc 1:848–858

Wang S, Hu Y, Tan W, Wu X, Chen R, Cao J, Chen M, Wang Y (2012) Compatibility art of traditional Chinese medicine: from the perspective of herb pairs. J Ethnopharmacol 143:412–423

Wang Y, Wang M, Xu M, Li T, Fan K, Yan T, Xiao F, Bi K, Jia Y (2018) Nootkatone, a neuroprotective agent from Alpiniae Oxyphyllae Fructus, improves cognitive impairment in lipopolysaccharide-induced mouse model of Alzheimer's disease. Int Immunopharmacol 62:77–85

Wei B, Liu MY, Chen ZX, Wei MJ (2018) Schisandrin ameliorates cognitive impairment and attenuates Aβ deposition in APP/PS1 transgenic mice: involvement of adjusting neurotransmitters and their metabolite changes in the brain. Acta Pharmacol Sin 39:616–625

Xu Z et al (2016) Total Lignans of Schisandra chinensis ameliorates Aβ1-42-induced neurodegeneration with cognitive impairment in mice and primary mouse neuronal cells. PLoS One 11:e0152772

Youn H, Ji I, Ji HP, Markesbery WR, Ji TH (2007) Under-expression of Kalirin-7 increases iNOS activity in cultured cells and correlates to elevated iNOS activity in Alzheimer's disease hippocampus. Journal of Alzheimers Disease Jad 12:271–281

Zhang GX et al (2013) [the role of TLR4-mediated MyD88-dependent pathway in neuroinflammation in hippocampal neurons of rats]. Chinese. J Appl Physiol 29:42